

Stellar Atmospheres Near an AGN: The Importance of Radiation Pressure from Trapped Lyman- α Photons

Weihsueh A. Chiu

Joseph Henry Laboratories, Department of Physics, Princeton, NJ 08544

and

B. T. Draine

Princeton University Observatory, Princeton, NJ 08544

Submitted to *The Astrophysical Journal*

ABSTRACT

We derive an analytic expression for the intensity of resonance-line radiation “trapped” in a semi-infinite medium. Given a source function and destruction probability per scattering, the radiation pressure due to trapped photons can be calculated by numerically integrating over analytic functions. We apply this formalism to a plane-parallel model stellar atmosphere to calculate the radiation pressure due to Lyman- α photons produced following absorption of UV and X-rays from an AGN. For low surface gravity stars near the AGN ($g \sim 10 \text{ cm s}^{-2}$, $r \sim 0.25 \text{ pc}$), we find that the pressure due to Lyman- α photons becomes an appreciable fraction of that required for hydrostatic support. If the broad emission line emitting gas in AGNs and QSOs consists of stellar outflows, it may be driven, in part, by Lyman- α pressure.

Subject headings: galaxies: active — line: formation — radiative transfer — stars: atmospheres

1. Introduction

Interest in the effect of hard UV and X-ray radiation on stellar atmospheres and stellar evolution began in earnest with work on X-ray binaries (e.g., Davidson & Ostriker 1973, Basko & Sunyaev 1973, and Arons 1973), but the subject has since been revisited in the context of active galactic nuclei (AGN).

Consider a star of effective temperature T_{eff} and an AGN of luminosity $L = 10^{46} L_{46} \text{ erg s}^{-1}$. The incident power per area from the AGN is equal to σT_{eff}^4 at the “heating” distance

$$d_h = \left(\frac{L}{4\pi\sigma T_{\text{eff}}^4} \right)^{1/2} = 1.5 \times 10^{17} L_{46}^{1/2} \left(\frac{5000\text{K}}{T_{\text{eff}}} \right)^2 \text{ cm}; \quad (1)$$

heating of the stellar surface by the AGN is important at distances $d \lesssim d_h$. Fabian (1979) was apparently the first to suggest that heating by AGN radiation might substantially affect the envelopes of nearby stars, resulting in enhanced mass loss. Edwards (1980) argued that when a star approached within $d \lesssim d_h$, the irradiated photosphere would develop supersonic horizontal winds carrying heat from the illuminated hemisphere to the shadowed side. Edwards conjectured that enhanced mass loss could then occur, resulting in a “cometary star” as the stellar outflow is accelerated radially away from the AGN. Matthews (1983) noted the importance of direct radiation pressure from the AGN, arguing that this could ablate matter tangentially from the stellar photospheres of giant or supergiant stars.

Voit & Shull (1988) discussed the effects of X-rays on the upper atmosphere of a star near the AGN. They argued that X-ray heating of a $\sim 1M_\odot$, $R_* \approx 100R_\odot$ star ($g \approx 3 \text{ cm s}^{-2}$) would result in a hot, ionized wind, with temperature at the critical point $T \approx 3 \times 10^5 \text{ K}$; radiation pressure in C IV, N V, and O VI resonance lines would contribute to the acceleration of the wind. They concluded that stars which are already red supergiants could develop winds with $\dot{M} \approx 10^{-7} L_{46}^{0.9} d_{18}^{-2} R_{*,100}^2 M_\odot \text{ yr}^{-1}$, where the distance from the AGN is $d = 10^{18} d_{18} \text{ cm}$, and $R_{*,100} \equiv R_*/100R_\odot$. These mass loss rates exceed normal mass loss rates for red supergiants only within a distance of $d_{18} \lesssim 0.3 L_{46}^{0.45} R_{*,100} \text{ cm}$. They estimated the mass loss due to ablation by radiation pressure (Matthews 1983) for a $\sim 1M_\odot$ star to be $\dot{M} \approx 10^{-8} L_{46} d_{18}^{-2} R_{*,100}^{5/2}$ provided $d_{18} < 0.6 L_{46}^{1/2} R_{*,100}$.

There has also been some exploration of how AGN radiation might affect the evolution of stars (Matthews 1983; Verbunt, Fabian, & Rees 1984; Tout et al. 1989). Tout et al. discussed the evolution of stars immersed in a blackbody background with temperature $T = 10^{3.75-4} \text{ K}$, concluding that the main sequence evolution is largely unaffected, but that the star will expand to a radius ~ 10 times larger than usual during the “red giant” phase of evolution. Note, however, that the energy density of AGN radiation equals a 10^4 K blackbody at a distance of only $2 \times 10^{16} L_{46}^{0.5} \text{ cm}$ from the AGN. Furthermore, it is not clear how their conclusions would have to be modified for the anisotropic and nonthermal radiation field of the AGN.

These discussions of the effects of AGN radiation on stellar atmospheres and evolution have led some to consider a “bloated stars scenario” (BSS) to explain the origin of the AGN broad line region (BLR). The BSS proposes that the BLR consists of the stellar winds and/or expanded envelopes of stars irradiated with AGN radiation (e.g., Penston 1988, Kazanas 1989). The attractiveness of this scenario stems from its efficient use of known resources: stars are believed to be present near the “central engines” of AGN, their gravity provides a possible “containment” mechanism for BLR clouds, there is ample mass with which to replenish the clouds, and the mass shed provides material to fuel the AGN. So far, however, no specific model has successfully explained how all these mechanisms might function, though pieces of the puzzle have been explored (Alexander & Netzer 1994). High signal/noise measurements of line profiles indicate that the number of discrete clouds or bloated stars must be large, perhaps exceeding $\sim 3 \times 10^6$ for Mrk 335

(Arav et al. 1997) and $\sim 3 \times 10^7$ for NGC 4151 (Arav et al. 1998). Such large numbers appear to challenge the BSS, but the difficulties may not be insurmountable.

Recent observations and photoionization models of Baldwin et al. (1996) and Ferland et al. (1996) offer some concrete evidence for the BSS. They find that the BLR seems to contain several distinct components. One (component “A”) has sharp (FWHM $\approx 1000 \text{ km s}^{-1}$), symmetric line profiles centered on zero velocity, while another (component “B”) appears to be outward-flowing, peaked at zero velocity but with a long blue tail (down to $-11,000 \text{ km s}^{-1}$). They interpret “A” as the expanded envelopes of stars, and “B” as their radiatively accelerated, outflowing winds.

The aim of the present paper is to call attention to the fact that irradiation of a star by hard X-rays from the AGN will result in the generation of Lyman- α ($\text{Ly}\alpha$) photons within the stellar atmosphere, and the pressure of these trapped resonance-line photons may contribute to mass loss. The possible importance of $\text{Ly}\alpha$ photons was suggested previously by Puetter [unpublished, cited in Penston (1988) and Voit & Shull (1988)]. Voit & Shull rejected Puetter’s suggestion, arguing that the $\text{Ly}\alpha$ pressure could be estimated to be

$$P_{\text{Ly}\alpha} \approx \left(\frac{aT^4}{3} \right) \frac{W_\lambda}{\lambda} \quad (2)$$

where W_λ is the equivalent width of the $\text{Ly}\alpha$ absorption profile of the gas between the point of interest and the surface, and T is the gas temperature. Voit & Shull then used $W_\lambda/\lambda < 1$ to obtain an upper limit $P_{\text{Ly}\alpha} \lesssim aT^4/3$ which, for stars of interest, is insufficient to “bloat” the atmosphere. However equation (2) presumes the radiation field within the gas to be close to a blackbody at the gas temperature T — an assumption which need not be valid when $\text{Ly}\alpha$ photons are being generated within the gas by nonthermal processes, such as $\text{H}(1s \rightarrow 2p)$ excitation by photoelectrons and secondary electrons in a non-Maxwellian “tail” to the electron energy distribution function. It is therefore essential to estimate the rate of production of $\text{Ly}\alpha$ photons, and to examine their diffusion in physical space and frequency space as well as the possibility of photon “destruction” by, for instance, collisional de-excitation of electronically excited H atoms.

In §2, we give a brief treatment of resonance-line transfer, extending the detailed calculations of Neufeld (1990). In particular, we derive an expression for the case of a semi-infinite, absorbing slab of material. Since resonance-line photons created in a stellar atmosphere will almost certainly not be able to scatter through the entire star without being absorbed, this limit is an excellent approximation. In §3, we apply our calculational method to a simple, plane parallel, irradiated model atmosphere. In §4, we present the results. In §5 we summarize and discuss implications and further directions for work.

2. Resonance Radiation Transfer

Most current photoionization treatments, including CLOUDY (Ferland 1996), use the escape probability approximation to address resonance-line radiation transfer. For example, Elitzur and

Ferland (1986) use the escape probability approximation (EPA) to derive the frequency-integrated radiation intensity $\mathcal{J}_{ul, \text{EPA}}$ for a resonance line at frequency ν_{ul} , corresponding to a transition from level u to level l , to be

$$\mathcal{J}_{ul, \text{EPA}} = B(\nu_{ul}, T_{\text{exc}})\Delta\nu_{ul}, \quad (3)$$

where $B(\nu_{ul}, T_{\text{exc}})$ is the Planck function at the line excitation temperature (which is calculated from the level populations) and $\Delta\nu_{ul}$ is the line width. The radiation pressure $P_{ul, \text{EPA}}$ is given, as usual, by

$$P_{ul, \text{EPA}} = \frac{4\pi}{3c}\mathcal{J}_{ul, \text{EPA}}. \quad (4)$$

In this purely local treatment, the escape probability approximation assumes that a resonance photon at a point r has a probability p_{ul} per scattering of “escaping” to a defined boundary r_0 , where it is assumed photons free-stream to infinity. Thus, the differential radiation pressure $P_{ul, \text{EPA}}^{\text{diff}}(r)$ at any point r is given by

$$P_{ul, \text{EPA}}^{\text{diff}}(r) \equiv P_{ul, \text{EPA}}(r) - P_{ul, \text{EPA}}(r_0) \quad (5)$$

$$= P_{ul, \text{EPA}}(r) \times (1 - p_{ul}) \quad (6)$$

$$= \frac{4\pi}{3c}B(\nu_{ul}, T_{\text{exc}})\Delta\nu_{ul}(1 - p_{ul}). \quad (7)$$

Confusingly, it is this *differential* radiation pressure which Elitzur and Ferland (1986) and CLOUDY (Ferland 1996) refer to as the “line radiation pressure.” We will always use the term “pressure” and the symbol P_i for the physical pressure (momentum flux) at point r due to particles i , such as gas particles or resonance line photons. We will use the term “differential pressure” and the symbol $P_i^{\text{diff}} \equiv P_i(r) - P_i(r_0)$ for the pressure difference due to particles i between the point of interest r and the boundary point r_0 .

Elitzur and Ferland (1986) note that the line width $\Delta\nu_{ul}$ is the “crucial parameter” in this calculation of the radiation pressure. In particular, it is not well understood how to calculate $\Delta\nu_{ul}$ at extremely large optical depths when the escape probability is comparable to the “destruction probability” per scattering, for example due to collisional de-excitation.

However, the case of very large optical depth is precisely that which Neufeld (1990) considers using a completely different approach. He presents in §§2–3 of his paper an *exact* and *analytic* calculation derived from Fourier transforming a diffusion equation. He solves this equation for a unit delta-function photon source in a uniform, optically thick (but finite) slab, with and without a finite destruction probability. In particular, at optical depth τ with a source at τ_s , the angle-averaged intensity $J(\tau, \tau_s, x)$ and frequency-integrated intensity $\mathcal{J}(\tau, \tau_s)$ are given in terms of infinite series [e.g., his equation (2.7)]. Unfortunately, these series converge rather slowly. However, we show below that if we take the limit of a semi-infinite slab, then the angle-averaged intensity $J(\tau, \tau_s, x)$ can be expressed in terms of analytic functions which can be integrated numerically with relative ease. Below, we first present the notational conventions we use, and then proceed with our derivation of the intensities J and \mathcal{J} in the case of a semi-infinite slab.

Neufeld (1990) defines a as the ratio of the natural line width to the Doppler width and τ as the mean optical depth:¹

$$a = \frac{\gamma}{4\pi} \frac{\lambda_0}{\sqrt{2} v_{1d}}, \quad \tau = \sigma_\alpha N_0, \quad \sigma_\alpha \equiv \frac{\pi e^2 f_{lu} \lambda_0}{m_e c \sqrt{2} v_{1d}} \quad (8)$$

where γ is the decay rate, λ_0 is the line-center wavelength, $v_{1d} = \sqrt{kT/m_H}$ is the one-dimensional velocity dispersion, m_H is the mass of atomic hydrogen, f_{lu} is the oscillator strength, m_e is the electron mass, N_0 is the column density of absorbers, and the other symbols have their usual meanings. For Ly α , this corresponds to $v_{1d} = 9.082 T_4^{1/2} \text{ km s}^{-1}$, $a = 4.717 \times 10^{-4} T_4^{-1/2}$, and $\tau = 1.045 \times 10^{-13} T_4^{-1/2} N_0 \text{ cm}^2$, where T_4 is the temperature in units of 10^4 K . The dimensionless frequency variables x and $\sigma(x)$ which Neufeld uses are given by:

$$x \equiv \frac{\lambda_0(\nu - \nu_0)}{\sqrt{2} v_{1d}}, \quad \sigma(x) \equiv \sqrt{\frac{2}{3}} \int_0^x \frac{dx'}{\phi(x')}, \quad (9)$$

where $\phi(x)$ is the Voigt profile normalized such that $\int \phi(x) dx = 1$. In this convention, $\phi(x)$ takes on the limits

$$\phi(0) = \frac{1}{\sqrt{\pi}} (1 + O(a)); \quad \phi(x) \approx \frac{a}{\pi x^2}, x \gg 1. \quad (10)$$

The intensity $J(\tau, \tau_s, x)$ is given per unit frequency in x , so that the frequency-integrated intensity is given by

$$\mathcal{J}(\tau, \tau_s) \equiv \int J(\tau, \tau_s, x) dx. \quad (11)$$

Since Neufeld's solutions for the intensities $J(\tau, \tau_s, x)$ and $\mathcal{J}(\tau, \tau_s)$ are derived for a delta-function source, they act as Green's functions for resonant photon sources. Consider a slab of total thickness τ_0 . For a Ly α emissivity per unit volume $4\pi j$, we define the injected power per unit area per unit optical depth as

$$\xi(\tau_s) = \frac{4\pi j(\text{Ly}\alpha)}{n(\text{H}^0)\sigma_\alpha}. \quad (12)$$

The excitation temperature T_{exc} at optical depth τ is found by integrating J near line center over all source locations τ_s , weighted by ξ , to obtain the total intensity at line center, and comparing with a blackbody intensity:

$$B(\nu_0, T_{\text{exc}}) \frac{d\nu_0}{dx} = \int_0^{\tau_0} \xi(\tau_s) J(\tau, \tau_s, 0) d\tau_s, \quad (13)$$

where $B(\nu_0, T_{\text{exc}})$ is the usual Planck function at the excitation temperature T_{exc} , evaluated at line center. Since the majority of scatterings occur near line center, the local level population for Ly α should be given by

$$\frac{n_{2p}}{n_{1s}} = \frac{g_{2p}}{g_{1s}} \exp\left(-\frac{\chi_{21}}{kT_{\text{exc}}}\right), \quad (14)$$

¹ For consistency, we retain the definitions of τ and σ_α used by Neufeld (1990), Harrington (1973), and other workers: $\sigma_\alpha = \sqrt{\pi}\sigma_o$, where σ_o is the absorption cross section at line-center.

where the n 's are the level populations, g 's are the statistical weights, and $\chi_{21} = 10.2 \text{ eV}$. The radiation pressure $P_{\text{rad}}(\tau) = 4\pi\mathcal{J}/(3c)$ is given similarly by

$$P_{\text{rad}}(\tau) = \frac{4\pi}{3c} \int_0^{\tau_0} \xi(\tau_s) \mathcal{J}(\tau, \tau_s) d\tau_s. \quad (15)$$

Consider photons created at line center with a constant probability per scattering $\epsilon_0 \ll 1$ that the photon will be “destroyed” by, for instance, collisional de-excitation. Using Neufeld’s equations (2.7) and (3.11)–(3.13), we find that for a slab of total thickness τ_0 and source at $0 \leq \tau_s \leq \tau_0$, the angle-averaged intensity at $0 \leq \tau \leq \tau_0$ can be written as

$$J(\tau, \tau_s, x) = \frac{\sqrt{6}}{8\pi^2} \left\{ F[\tau - \tau_s, \sigma(x)] - F\left[\tau + \tau_s + \frac{4}{3\phi(x)} + O(\tau_0^{-1}), \sigma(x)\right] \right\}, \quad (16)$$

$$F[v, \sigma(x)] \equiv \frac{\pi}{\tau_0} \sum_{n=1}^{\infty} \frac{\cos(\mu_n v)}{\mu_n + \epsilon_0 \sqrt{6}/2} \exp[-\mu_n |\sigma(x)|], \quad (17)$$

$$\mu_n = \frac{n\pi}{\tau_0} \left[1 + O(\tau_0^{-1}) \right]. \quad (18)$$

Note that our τ_0 is *twice* Neufeld’s τ_0 .

In a stellar atmosphere, we essentially have a semi-infinite slab, where $\tau_0 \rightarrow \infty$. We can therefore neglect the terms of order τ_0^{-1} , and replace the sum in equation (17) with an integral. With the substitutions

$$\tau_d \equiv \frac{2}{\epsilon_0 \sqrt{6}}, \quad (19)$$

$$u_n \equiv \tau_d \mu_n = n\pi\tau_d/\tau_0, \quad \frac{du_n}{dn} = \pi\tau_d/\tau_0, \quad (20)$$

F then becomes

$$F(v, \sigma) \rightarrow \int_0^{\infty} \frac{\cos(uv/\tau_d)}{1+u} \exp[-u|\sigma(x)|/\tau_d] du \quad (21)$$

$$= \mathcal{E}(z) \equiv \text{Re}[e^z E_1(z)], \quad (22)$$

$$z \equiv \frac{|\sigma(x)| + i|v|}{\tau_d}, \quad (23)$$

where $E_1(z) \equiv \int_z^{\infty} w^{-1} e^{-w} dw$ is the exponential integral with complex argument. The quantity τ_d is the effective optical depth due to finite destruction probability.

Therefore, the angle-averaged intensity in the limit that $\tau_0 \rightarrow \infty$ is given by

$$J(\tau, \tau_s, x) = \frac{\sqrt{6}}{8\pi^2} \left\{ \mathcal{E}\left[\frac{|\sigma(x)| + i|\tau - \tau_s|}{\tau_d}\right] - \mathcal{E}\left[\frac{|\sigma(x)| + i|\tau + \tau_s + \frac{4}{3\phi(x)}|}{\tau_d}\right] \right\}. \quad (24)$$

At line center, where $x = \sigma = 0$ and the argument z is purely imaginary, $\mathcal{E}(z)$ can be expressed in terms of cosine and sine integrals $\text{Ci}(y) \equiv -\int_y^{\infty} t^{-1} \cos t dt$ and $\text{si}(y) \equiv -\int_y^{\infty} t^{-1} \sin t dt$:

$$\mathcal{E}(iy) = -[\cos y \text{Ci}(y) + \sin y \text{si}(y)]. \quad (25)$$

Using equations (24)–(25) in equation (13) gives the excitation temperature, and hence the level population at each point in the slab using equation (14).

To find the frequency-integrated intensity \mathcal{J} , we must integrate J over the frequency x , equation (11). The exact expression for the frequency-integrated intensity in the limit that $\tau_0 \rightarrow \infty$ is thus:

$$\mathcal{J}(\tau, \tau_s) = \frac{\sqrt{6}}{8\pi^2} \left[\mathcal{F}_{\tau_d} (|\tau - \tau_s|) - \mathcal{G}_{\tau_d} (\tau + \tau_s) \right], \quad (26)$$

$$\mathcal{F}_{\tau_d}(v) \equiv 2 \times \int_0^\infty \mathcal{E} \left[\frac{\sigma(x) + iv}{\tau_d} \right] dx, \quad (27)$$

$$\mathcal{G}_{\tau_d}(v) \equiv 2 \times \int_0^\infty \mathcal{E} \left[\frac{\sigma(x) + i \left(v + \frac{4}{3\phi(x)} \right)}{\tau_d} \right] dx. \quad (28)$$

The functions \mathcal{F} and \mathcal{G} in general need to be calculated numerically. Obtaining the numerical integral is simplified by taking into account the following limits of the integrand:

$$\mathcal{E} \left[\frac{\sigma(x) + iv}{\tau_d} \right] \propto \begin{cases} \sim \text{constant} & \text{if } x \lesssim (av)^{1/3} \text{ and } x \lesssim (a\tau_d)^{1/3}; \\ \sim x^3 & \text{if } (a\tau_d)^{1/3} \lesssim x \lesssim (av)^{1/3} \text{ and } \tau_d < v; \\ \sim x^{-3} & \text{if } x \gtrsim (a\tau_d)^{1/3} \text{ and } x \gtrsim (av)^{1/3}. \end{cases} \quad (29)$$

If the Ly α optical depths τ and τ_s , as well as the effective optical depth to destruction τ_d , are all large, so that $(av)^{1/3} \gg 1$ and $(a\tau_d)^{1/3} \gg 1$, then the scattering is dominated by the damping wings. We may then approximate the Voigt profile $\phi(x)$ by using equation (10) and $\sigma(x)$ by $\sigma(x) \approx \sqrt{2/3} \pi x^3 / (3a)$. This approximation leads to an *analytic* expression for \mathcal{F} and \mathcal{G} :

$$\mathcal{F}_{\tau_d}(v) \approx \frac{2\sqrt{3}}{3} \Gamma(1/3) \Gamma(2/3) \left(\frac{a\tau_d}{\sqrt{2}\pi} \right)^{1/3} \text{Re} [\exp(iv/\tau_d) \Gamma(1/3, iv/\tau_d)] \quad (30)$$

$$\mathcal{G}_{\tau_d}(v) \approx \mathcal{F}_{\tau_d} \left[v + \frac{4}{3\phi(0)} \right], \quad (31)$$

where the incomplete gamma function with an imaginary argument is $\Gamma(b, iy) \equiv i^b \int_y^\infty t^{b-1} e^{-it} dt$. This case is not applicable to the AGN-illuminated stellar atmosphere model we discuss below, but we include it for completeness.

3. A Stellar Atmosphere Near an AGN

Our procedure for evaluating the importance of Ly α pressure in a stellar atmosphere near an AGN is as follows:

- A. Use a slightly-modified version of CLOUDY (Ferland 1996) to calculate the thermal and ionization structure of a plane-parallel, gravitationally confined gas illuminated by an AGN.

- B. Calculate the Ly α production and destruction rates from A.
- C. Use B and the analytic model from §2 to calculate the Ly α radiation pressure $P_{\text{Ly}\alpha}(r)$.
- D. Compare the differential radiation pressure $P_{\text{Ly}\alpha}^{\text{diff}} \equiv P_{\text{Ly}\alpha}(r) - P_{\text{Ly}\alpha}(r_0)$ from C with P_{hyd} , the pressure required for hydrostatic equilibrium.

If $P_{\text{Ly}\alpha}^{\text{diff}} \approx \frac{1}{2}P_{\text{hyd}}$, then the atmosphere may be unstable, especially since other resonance lines will likely contribute to the total radiation pressure (Elitzur & Ferland 1986). We describe each of these steps in greater detail below.

3.1. Use of CLOUDY

We have modified the CLOUDY program (version 90.02) of Ferland (1996) to model a plane-parallel atmosphere with a constant gravitational acceleration, aligned normal to the incident AGN flux. We ignore the radiation from the star, considering only the effect of the AGN illumination on a gravitationally confined gas. The modifications to CLOUDY thus only involve adding a constant gravitational acceleration g to the equation for the total pressure equilibrium:

$$P_{\text{tot}}(r) \equiv P_{\text{gas}}(r) + P_{\text{lines}}(r) = \int_r^{r_0} [a_{\text{cont}}(r) + g]\rho(r)dr + P_{\text{gas}}(r_0) + P_{\text{lines}}(r_0). \quad (32)$$

Here r is the distance from the center of the star, r_0 is the starting point of the integration ($r \leq r_0$), $P_{\text{gas}}(r)$ and $P_{\text{lines}}(r)$ are the pressures due to gas and resonance lines respectively (the latter calculated by CLOUDY using escape probabilities), and $\rho(r)$ is the gas mass density. We define the hydrostatic pressure P_{hyd} to be the total pressure P_{tot} minus the free-streaming radiation pressure at r_0 , $P_{\text{lines}}(r_0)$:

$$P_{\text{hyd}}(r) \equiv P_{\text{tot}}(r) - P_{\text{lines}}(r_0). \quad (33)$$

This hydrostatic pressure provides the basis of comparison with the differential radiation pressure $P_{\text{lines}}^{\text{diff}}$, since it is the equivalent gas pressure necessary for hydrostatic equilibrium, in the absence of any line radiation pressure. The acceleration due to the momentum deposition from the attenuation of the AGN continuum flux is given by

$$a_{\text{cont}}(r) = \frac{1}{c\mu_{\text{H}}m_{\text{H}}} \int_{-\infty}^{\infty} \sigma_{\nu}^{\text{eff}}(r)f_{\nu}(r)d\nu, \quad (34)$$

where μ_{H} is the gas mass per H nucleon in units of the mass of atomic hydrogen m_{H} , $f_{\nu}(r)$ is the AGN energy flux per unit frequency, and $\sigma_{\nu}^{\text{eff}}(r)$ is the effective cross section per H nucleon, the latter two quantities evaluated at frequency ν and distance r . Recall that the line radiation pressure calculated by CLOUDY $P_{\text{Ly}\alpha}^{\text{CLOUDY}}(r)$ is actually the differential line radiation pressure $P_{\text{Ly}\alpha}^{\text{diff}}(r)$. Our treatment, on the other hand, explicitly calculates both $P_{\text{Ly}\alpha}(r)$ and $P_{\text{Ly}\alpha}(r_0)$,

the momentum flux in free-streaming resonance photons at r_0 , and takes their difference to find $P_{\text{Ly}\alpha}^{\text{diff}}(r)$.

The abundances we use are those used by Ferland et al. 1996 and Baldwin et al. 1996: $\log_{10}(\text{H: He: Li: Be: B: C: N: O: F: Ne: Na: Mg: Al: Si: P: S: Cl: Ar: K: Ca: Sc: Ti: V: Cr: Mn: Fe: Co: Ni: Cu: Zn}) = (0: -0.907: -7.92: -9.82: -8.35: -3.08: -2.94: -2.23: -6.71: -3.10: -4.87: -3.6: -4.71: -3.64: -5.62: -3.97: -5.92: -4.63: -6.06: -4.85: -8.76: -6.91: -7.83: -6.16: -6.31: -4.18: -8.5: -5.6: -7.58: -7.19)$. The incident AGN flux we use is the same one used by Baldwin et al. 1996 and Ferland et al. 1996 in their photoionization models of the BLR. Their formula is equivalent to

$$\begin{aligned} \nu f_{\nu}^0 &= \frac{\nu L_{\nu}}{4\pi d^2} = \frac{A}{4\pi d^2} \left(\frac{\nu}{\nu_0} e^{-\nu/\nu_c} + 0.09 e^{-\nu_0/\nu} \right) \\ h\nu &\leq E_{\text{max}} \end{aligned} \quad (35)$$

where $h\nu_c = 21.5$ eV and $h\nu_0 = 13.6$ eV, which corresponds to a UV–X-ray spectral index $\alpha_{ox} = -1.2$. For a Hubble’s constant $H_0 = 65 h_{65} \text{ km s}^{-1} \text{ Mpc}^{-1}$, Baldwin et al. (1996) adopt $A = 1.77 \times 10^{47} h_{65}^{-2} \text{ erg s}^{-1}$ and a distance of $d = 0.25 h_{65}^{-1} \text{ pc}$, both of which we adopt as well. We use a high energy cutoff of $E_{\text{max}} = 100$ keV. The luminosity in ionizing radiation is related to equation (35) by

$$L_{\text{ion}} \equiv \int_{\nu_0}^{\nu_{\text{max}}} L_{\nu} d\nu = 1.57 \cdot A. \quad (36)$$

Using L_{ion} as an estimate for the AGN luminosity heating of the star, we obtain using equation (1) a “heating distance” of

$$d_h \approx \left(\frac{L_{\text{ion}}}{4\pi\sigma T_{\text{eff}}^4} \right)^{1/2} = 0.26 \left(\frac{5000 \text{ K}}{T_{\text{eff}}} \right)^2 h_{65}^{-1} \text{ pc}. \quad (37)$$

Therefore, for a $T_{\text{eff}} = 5000$ K star, our calculations are at the heating distance.

Finally, a few notes about our integration procedure in CLOUDY. We begin our integration at a large distance with a total hydrogen density of 10^{10} cm^{-3} [which also determines $P_{\text{gas}}(r_0)$ in equation (32)] and an unattenuated incident flux (35); we integrate inward and stop when the electron fraction drops to 5%; and we iterate the solution until pressure equilibrium (with CLOUDY’s implementation of the resonance-line radiation pressure) is reached.

3.2. Calculation of Lyman- α Production and Destruction Rates

Given the ionization equilibrium calculated by CLOUDY, we calculate the Ly α production and destruction rates in the following manner. For Ly α production, we assume all electrons entering either $n = 2$ states which do not involve the absorption of a scattered Ly α photon result in the production of a *new* Ly α photon. We are justified in including electrons entering the

2s state, because at the densities we consider, an electron in the 2s state has an overwhelming probability of being collisionally transferred to the 2p state, and because once an electron is in the 2p state, the overwhelming probability is that it will result in the emission of a Ly α photon. Thus the production processes we consider include (1) radiative and collisional (3-body) recombination directly to $n = 2$, (2) photoexcitation by the AGN continuum, (3) collisional excitation by thermal electrons, (4) radiative and collisional de-excitation from $n > 2$, and (5) collisional excitation by photoelectrons and secondary electrons. This gives a Ly α production emissivity per unit volume, as a function of hydrogen column density N_{H} , of

$$4\pi j(N_{\text{H}}) = \chi_{21} n_{\text{H}} \sum_{j=1}^5 \Gamma_j(\rightarrow 2\text{p}, 2\text{s}) \quad (38)$$

where χ_{21} is 10.2 eV, n_{H} is the total hydrogen number density, Γ_j is the rate for process j per hydrogen nucleon. In Figure 1, we show the Ly α photon production rate per hydrogen nucleon [i.e., the summation in equation (38)] in the case of stellar atmospheres with $g = 1, 10, \text{ and } 100 \text{ cm s}^{-2}$.

The destruction probability ϵ_0 is the probability per scattering that either an electron in 2p does not end up producing a (scattered) Ly α photon, or that a scattered Ly α photon is absorbed by something other than an electron in the 1s state of hydrogen. Thus the processes we consider are (1) photo- and collisional ionization from 2p, (2) collisional de-excitation from 2p to 1s, (3) photo- and collisional excitation from 2p to $n > 2$, (4) absorption by the H $_2$ Lyman bands from $v = 2, J = 5, 6$, and (5) transition to 2s followed by (5a) two-photon decay to 1s, (5b) photo- and collisional ionization from 2s, (5c) collisional de-excitation from 2s to 1s, (5d) photo- and collisional excitation from 2s to $n > 2$. For molecular hydrogen, we use the rates and population fractions from Neufeld (1980, section V, *a, ii-iii*). We therefore obtain a destruction probability per scattering of:

$$\epsilon_0 = 1.2 \times 10^{-3} \frac{n_{\text{H}_2}}{n_{\text{H}}} + A_{21}^{-1} \times \left[\Gamma_1(2\text{p} \rightarrow) + \Gamma_2(2\text{p} \rightarrow) + \Gamma_3(2\text{p} \rightarrow) + \Gamma(2\text{p} \rightarrow 2\text{s}) \frac{\Gamma_{5\text{a}}(2\text{s} \rightarrow) + \Gamma_{5\text{b}}(2\text{s} \rightarrow) + \Gamma_{5\text{c}}(2\text{s} \rightarrow) + \Gamma_{5\text{d}}(2\text{s} \rightarrow)}{\Gamma(2\text{s} \rightarrow 2\text{p})} \right] \quad (39)$$

where the first term is due to molecular hydrogen, A_{21} is the Ly α decay rate, $\Gamma_i(2\text{p} \rightarrow)$ is the rate per 2p atom for process i , $\Gamma_i(2\text{s} \rightarrow)$ is the rate per 2s atom of process i , and $\Gamma(2\text{p} \rightarrow 2\text{s})$ and $\Gamma(2\text{s} \rightarrow 2\text{p})$ are the rates per 2p or 2s atom of transition to 2s or 2p, respectively. In Figure 2, we show the Ly α destruction probability per scattering which we calculate using equation (39) and the results of CLOUDY for $g = 1, 10, \text{ and } 100 \text{ cm s}^{-2}$. We note that we find Ly α destruction to be dominated by photo- and collisional ionization and excitation out of the $n = 2$ states.

4. Results of Calculation of Lyman- α Pressure

With the distribution of Ly α sources from equations (12) and (38), we numerically integrate equation (15) with equations (26)–(28) and (39) to determine $P_{\text{Ly}\alpha}$ in each layer.

For the incident flux $A/(4\pi d^2) = 1.77 \times 10^{47} h_{65}^{-2} \text{ erg s}^{-1}/[4\pi(0.25 h_{65}^{-1} \text{ pc})^2]$ estimated by Baldwin et al. 1996 and Ferland et al. 1996 (corresponding to a luminosity $L_{46} = 27.8 h_{65}^{-2}$), the only parameter that can be varied is the gravitational acceleration. We consider $g = 1, 10, 100 \text{ cm s}^{-2}$. The results are presented in Figures 3–5. It appears that for $g \lesssim 10 \text{ cm s}^{-2}$, the Ly α pressure rises to $\sim 10\%$ of the hydrostatic pressure. In this region, the total hydrogen column density $N_{\text{H}} \sim 10^{22} \text{ cm}^{-2}$. The gas number density is $n \sim 10^{11} \text{ cm}^{-3}$, below the estimate by Ferland et al. (1996) and Baldwin et al. (1996) of $n \sim 10^{12.5} \text{ cm}^{-3}$. We also show results for stellar atmospheres at $d = 0.125$ and $0.5 h_{65}^{-1} \text{ pc}$, corresponding to half and twice the heating distance, and obtain similar results. Our results are insensitive to changing the “boundary” hydrogen number density by a factor of ~ 10 . In Figure 6, we compare the $P_{\text{Ly}\alpha}^{\text{diff}}$ that we derive with that which CLOUDY calculates; note that the escape probability approximation used by CLOUDY tends to overestimate the radiation pressure, at least in the cases examined here.

As a check, we compare the excitation temperature derived from CLOUDY’s escape probability approximation with that derived from our own calculation using equation (13). The results, shown in Figure 7, are quite consistent, implying that the equilibrium level populations are well described by the escape probability approximation. Hence, it is the scattering in the damping wings of the line profile, which does not significantly affect the level population but which greatly affects the line width, which is inaccurately calculated by CLOUDY in the escape probability approximation. In comparing the excitation temperature to the kinetic temperature, we see from Figure 7 that there is a region of column density $\sim 10^{22} \text{ cm}^{-2}$ in which T_{exc} exceeds T_{kin} by a factor $\gtrsim 2$. Hence, the naive estimate of the radiation pressure using equation (2) may be as much as a factor of ~ 16 too small.

Our objective has been to carry out an exploratory investigation of the importance of Ly α pressure in the atmosphere of a star which is being irradiated by an AGN. This study has involved a number of simplifying approximations. In particular, we have treated the atmosphere as plane-parallel with normally-incident irradiation; this, of course, precludes examination of the important streaming effects which appear likely to ensue from the transverse pressure gradients which must arise from the non-uniform irradiation of the stellar surface.

In view of the neglect of the transverse pressure gradients and resulting motions, we have not iterated to a fully self-consistent solution. Our hydrostatic equilibrium is obtained using CLOUDY’s estimate for the radiation pressure rather than our more accurate result for $P_{\text{Ly}\alpha}$. Nor have we addressed the issue of stability or included radiation pressure from lines other than Ly α and from the star’s own luminosity.

With these numerous simplifications, we find that in low gravity stars, the differential pressure due to Ly α can rise to $\sim 10\%$ of the hydrostatic pressure.

5. Summary and Discussion

We have developed a formalism for computing the Ly α pressure in a plane-parallel stellar atmosphere. The treatment of resonance-line trapping given in §2 can be incorporated into already developed stellar atmosphere codes. For conditions believed representative of the BLR (ionizing flux of $\sim 4 \times 10^{10}$ erg cm $^{-2}$ s $^{-1}$), stars with $g \lesssim 10$ cm s $^{-2}$ will develop an appreciable pressure due to trapped Ly α photons in their atmospheres.

We have neglected numerous complicating factors, all of which appear likely to enhance the rate of mass loss. First of all, the gravitational acceleration $g \propto r^{-2}$, rather than the assumed $g = \text{constant}$. As a result, the outer layers of the atmosphere will have a larger scale height and must ultimately go over into a thermal wind, even if the lower layers are essentially hydrostatic and stable. With the outer layers of the atmosphere photoionized and heated to $T_4 \gtrsim 1$, a fluid element will have positive enthalpy at $r \gtrsim 600 T_4^{-1} (M/M_\odot) R_\odot$.

Furthermore, we have neglected the radiation pressure due to resonance lines other than Ly α , as well as the radiation from the star itself. Ferland (1997) reports that including radiation pressure from all resonance lines rather than just a select few sometimes increases the total radiation by an order of magnitude (using CLOUDY’s escape probability approximation, of course). Since no part of our derivation in §2 depends explicitly on the resonance line being Ly α , it is straight forward to extend our calculation to include other resonance lines.

Most important, however, is the fact that except along the “axis” — the line from the center of the star to the AGN — the atmosphere will be subject to substantial tangential stresses due to three effects related to anisotropic irradiation by the AGN:

1. The momentum deposited by absorbed photons — at anywhere other than the axis, the momentum will have a tangential component;
2. Transverse gradients in the Ly α pressure — at any particular radial column density N_H , the Ly α production rate will be greater along the axis, where X-rays are entering radially; and
3. Transverse gradients in the gas temperature — the rate of X-ray heating will be largest along the axis, where the zenith angle is zero.

These tangential stresses must result in significant tangential flows, with flow velocities that might approach escape speeds along the “terminator,” perhaps resulting in a “cometary star” as envisioned by Edwards (1980) and Matthews (1983).

It would obviously be of great interest to calculate axisymmetric fluid-dynamical models of red giant atmospheres subject to intense X-ray irradiation in order to investigate the effects of tangential stresses. It should be noted, of course, that we lack a quantitative theory for mass loss even from unperturbed evolved stars, so we are hardly poised to develop a definitive treatment including this new complication. Nevertheless, it does appear likely that trapped Ly α may help

drive mass loss in low- g stars subject to intense X-ray irradiation. The extra Ly α radiation pressure and associated tangential stresses might induce such evolving stars to “bloat” further and lose mass prematurely, so that the population of stars near the AGN core could be skewed from the average throughout the galaxy.

Finally, we note that none of our calculations are dependent on the gravitating object being a star. Recently, Walker and Wardle (1998) have suggested the existence of a population of cool, self-gravitating clouds in the galactic halo to account for “Extreme Scattering Events” which occur in monitoring the flux of compact radio sources. They propose clouds of approximately a Jovian mass with a radius of about an AU, which would correspond to a gravitational acceleration $g \sim 6 \times 10^{-4} \text{ cm s}^{-2}$ at the “surface.” With a total column density of $\sim 10^{26} \text{ cm}^{-2}$, the majority of the AGN energy flux would be absorbed well before reaching (and disrupting) the center of the cloud. The proposed particle number density of $\sim 10^{12} \text{ cm}^{-3}$ corresponds well to that inferred by Ferland et al. (1996) and Baldwin et al. (1996). Thus if these self-gravitating, sub-stellar clouds exist in host galaxies of AGN, they seem to be potential candidates for the origin of the BLR. It is unclear, though, how they could exist with a high metal content, as required by BLR observations, without rapidly cooling and collapsing (in much less than a Hubble time) prior to exposure to AGN irradiation.

Although we conclude that X-ray induced Ly α pressure would not be significant for main sequence stars near AGN, it could be important either for lower gravity stars which have evolved off the main sequence up the giant branch, or for substellar, self-gravitating clouds. It remains to be seen whether the resulting cometary structures can account for the required BLR covering factor and cloud population, and the AGN mass supply.

We gratefully acknowledge Bohdan Paczyński for useful and inspiring discussions, Gary Ferland for help and advice with CLOUDY, and R. H. Lupton for the availability of the SM plotting package. The research was supported in part by NSF grant AST-9619429.

REFERENCES

- Alexander, T., & Netzer, H. 1994, MNRAS, 270, 781
- Arav, N., Barlow, T. A., Laor, A., & Blandford, R. D. 1997, MNRAS, 288, 1015
- Arav, N., Barlow, T. A., Laor, A., Sargent, W. L. W., & Blandford, R. D. 1998, preprint (astro-ph/9801012)
- Arons, J. 1973 ApJ, 184, 539
- Baldwin, J. A., Ferland, G. J., Korista, K. T., Carswell, R. F., Hamann, F., Phillips, M. M., Verner, D., Wilkes, B. J., & Williams, R. E. 1996, ApJ, 461, 664

- Basko, M. M., & Sunyaev, R. A. 1973, *Ap. Space Sci.*, 23, 117
- Davidson, K., & Ostriker, J. P. 1973, *ApJ*, 179, 585
- Edwards, A. C. 1980, *MNRAS*, 190, 757
- Elitzur, M., & Ferland, G. J., 1986, *ApJ*, 305, 35
- Fabian, A. C. 1979, *Proc. Royal Soc. London A*, 366, 449
- Ferland, G. J., 1996, *Hazy, a Brief Introduction to Cloudy*, University of Kentucky Department of Physics and Astronomy Internal Report (available <http://www.pa.uky.edu/~gary/cloudy>)
- Ferland, G. J., Baldwin, J. A., Korista, K. T., Hamann, F., Carswell, R. F., Phillips, M. M., Wilkes, B. J., & Williams, R. E. 1996, *ApJ*, 461, 683
- Ferland, G. J., 1997, “CLOUDY 90 Revision History” web site, <http://www.pa.uky.edu/~gary/cloudy/c90rev.htm>
- Harrington, J. P., 1973, *MNRAS*, 162, 43
- Kazanas, D. 1989, *ApJ*, 347, 74
- Matthews, W. G. 1983, *ApJ*, 272, 390
- Neufeld, D. A. 1990, *ApJ*, 350, 216
- Penston, M. V. 1988, *MNRAS*, 233, 601
- Puetter, R. C. 1988
- Tout, C. A., Eggleton, P. P., Fabian, A. C., & Pringle, J. E. 1989, *MNRAS*, 238, 427
- Verbunt, F., Fabian, A. C., & Rees, M. J. 1984, *Nature*, 309, 331
- Voit, G. M., & Shull, J. M. 1988, *ApJ*, 331, 197
- Walker, M., & Wardle, M. 1998, preprint (astro-ph/9802111)

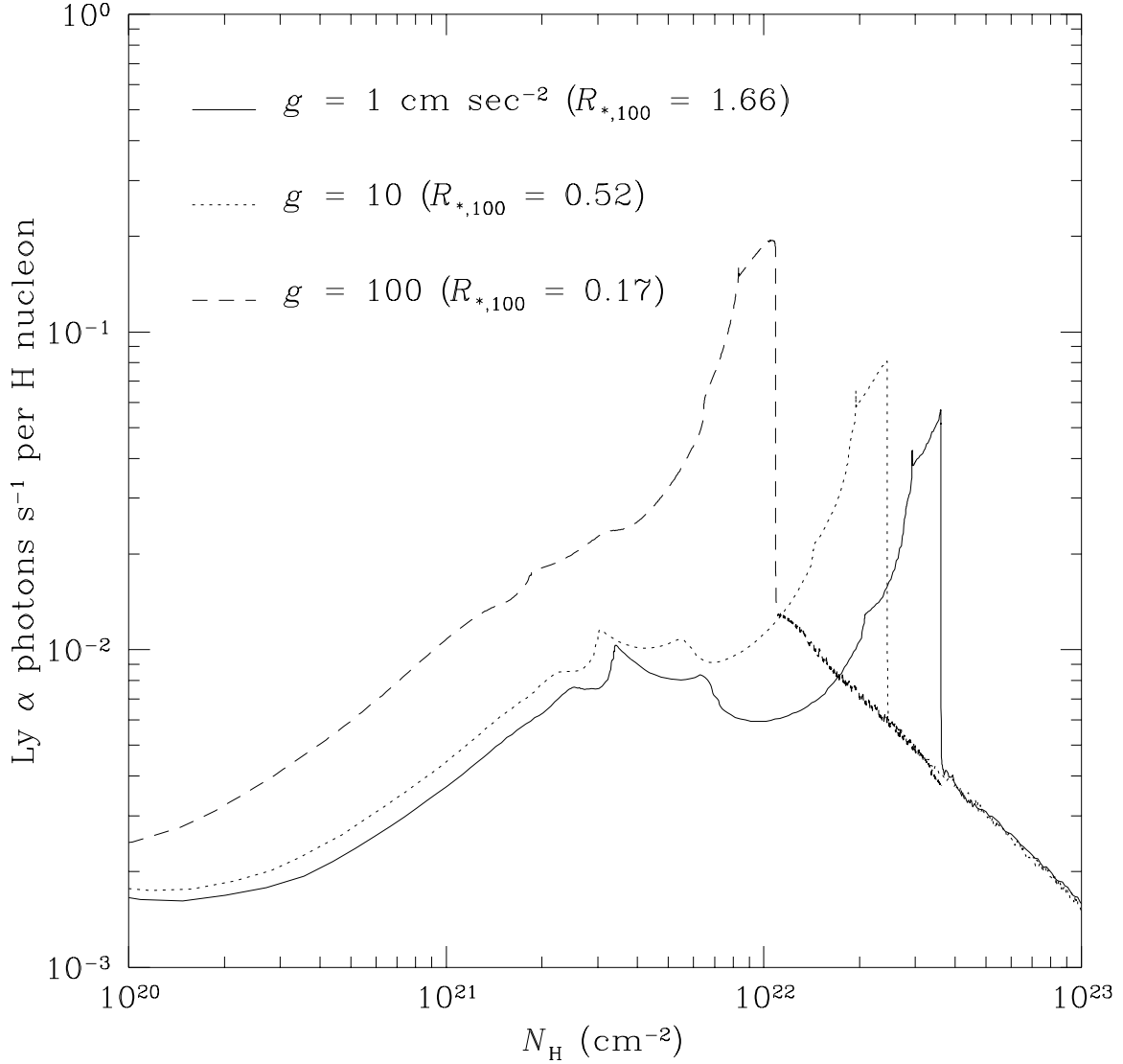


Fig. 1.— The Ly α photon injection rate per H nucleon as a function of total hydrogen column density N_{H} , in the cases of $g = 1, 10,$ and 100 cm s^{-2} . The incident flux is given by equation (35) with $A/(4\pi d^2) = 2.37 \times 10^{10} \text{ erg cm}^{-2} \text{ s}^{-1}$, corresponding to a distance $0.25 h_{65}^{-1} \text{ pc}$ from an AGN of luminosity $L_{46} = 27.8 h_{65}^{-2}$. The heating distance d_h for this value of L_{46} is $0.26 h_{65}^{-1} \text{ pc}$. The atmosphere is assumed to have $n_{\text{H}} = 10^{10} \text{ cm}^{-3}$ at $N_{\text{H}} = 0$. The stellar radius $R_{*,100}$ in units of $100R_{\odot}$ is given for each value of g , assuming a stellar mass of M_{\odot} .

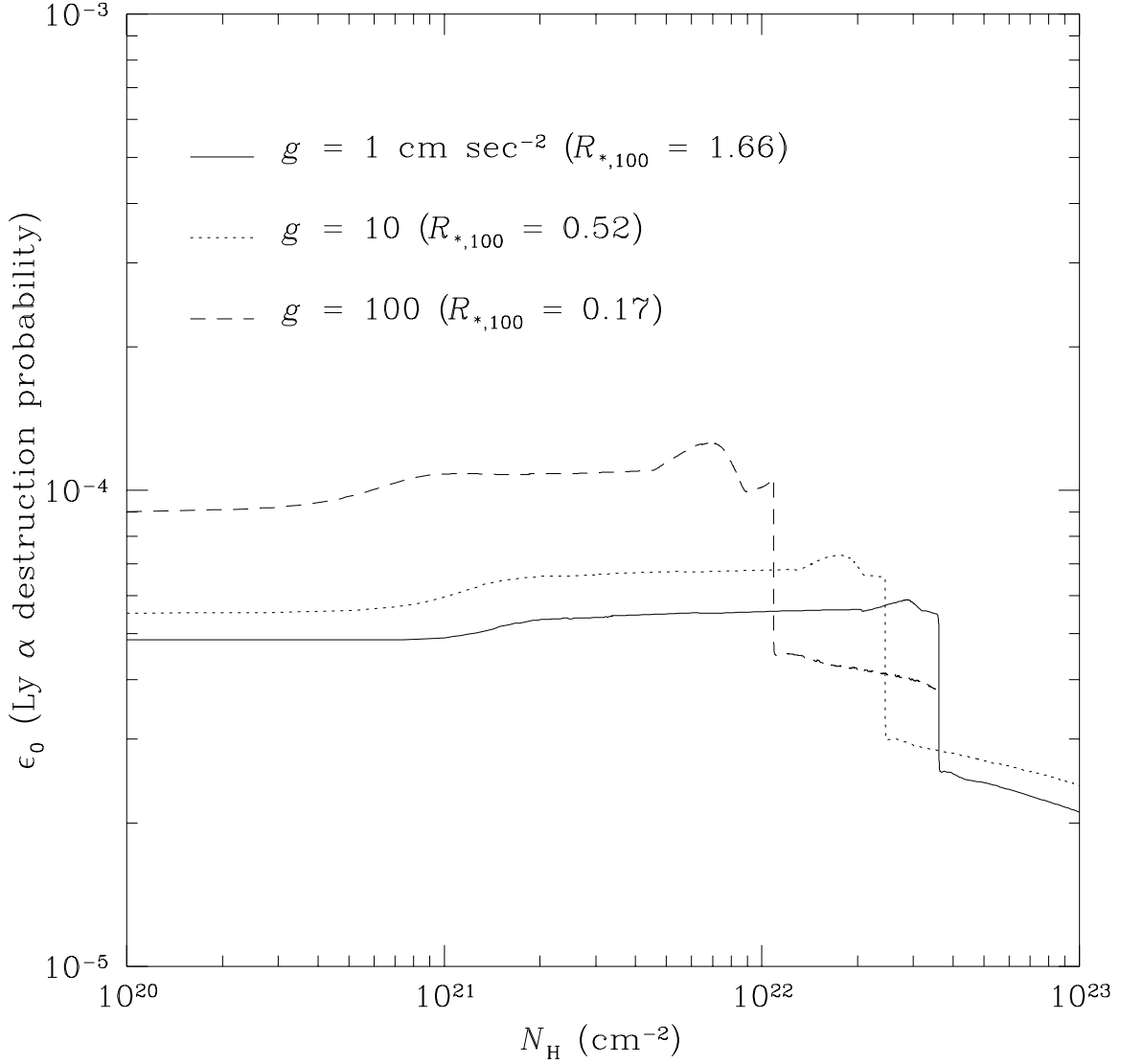


Fig. 2.— The Ly α photon destruction probability per scattering ϵ_0 as a function of total hydrogen column density N_{H} , calculated from equation (39), in the cases of $g = 1, 10,$ and 100 cm s^{-2} . The incident flux is given by equation (35) with $A/(4\pi d^2) = 2.37 \times 10^{10} \text{ erg cm}^{-2} \text{ s}^{-1}$.

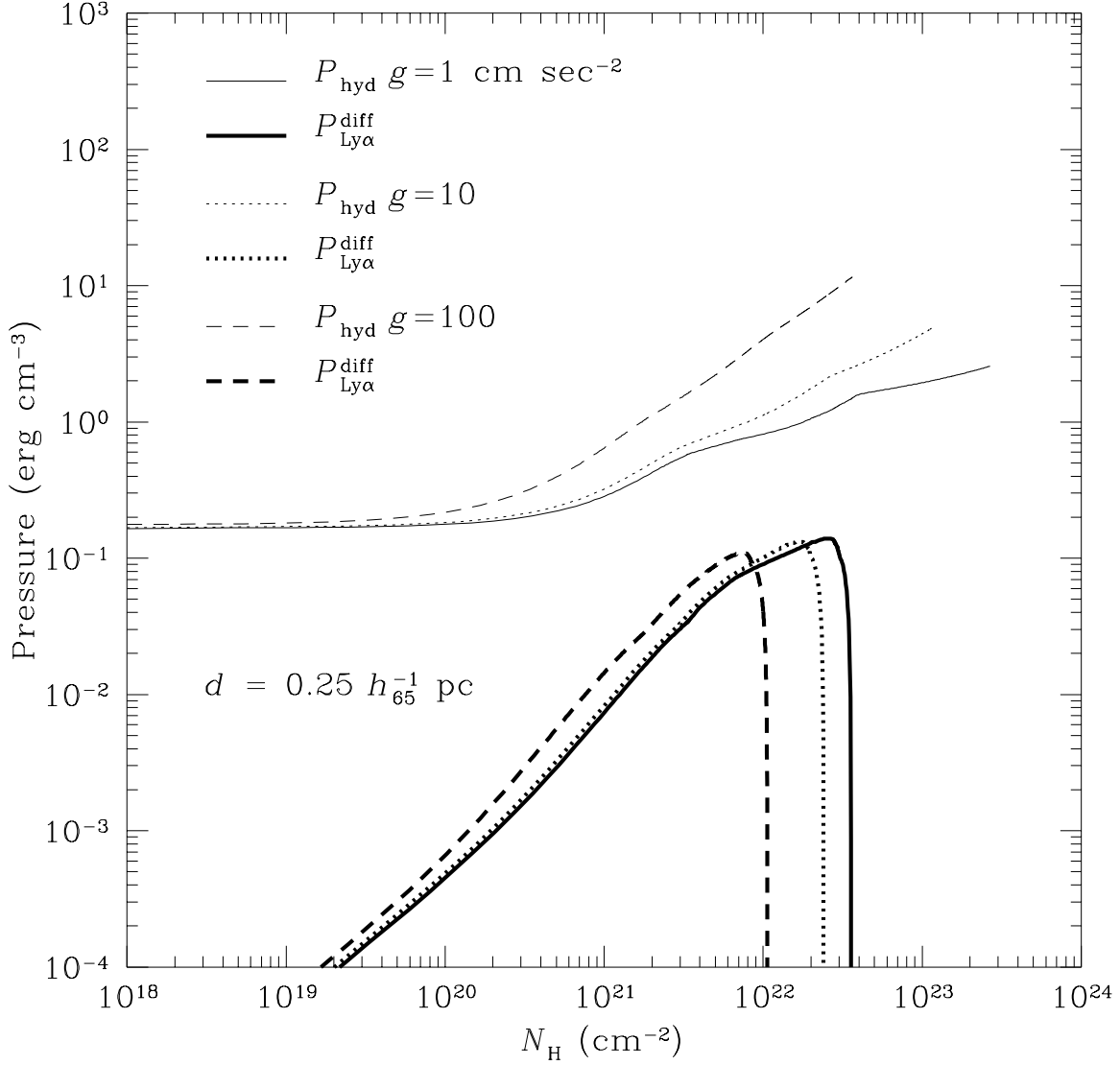


Fig. 3.— The differential radiation pressure $P_{\text{Ly}\alpha}^{\text{diff}}$ (thick lines) due to trapped Ly α photons is plotted as a function of total H column density N_{H} , for $g = 1, 10,$ and 100 cm s^{-2} . The incident flux is given by equation (35) with $A/(4\pi d^2) = 2.37 \times 10^{10} \text{ erg cm}^{-2} \text{ s}^{-1}$. The thin lines are the pressures required for hydrostatic support P_{hyd} at the same gravities [see equation (33)], where we have assumed a density $n_{\text{H}} = 10^{10} \text{ cm}^{-3}$ at $N_{\text{H}} = 0$.

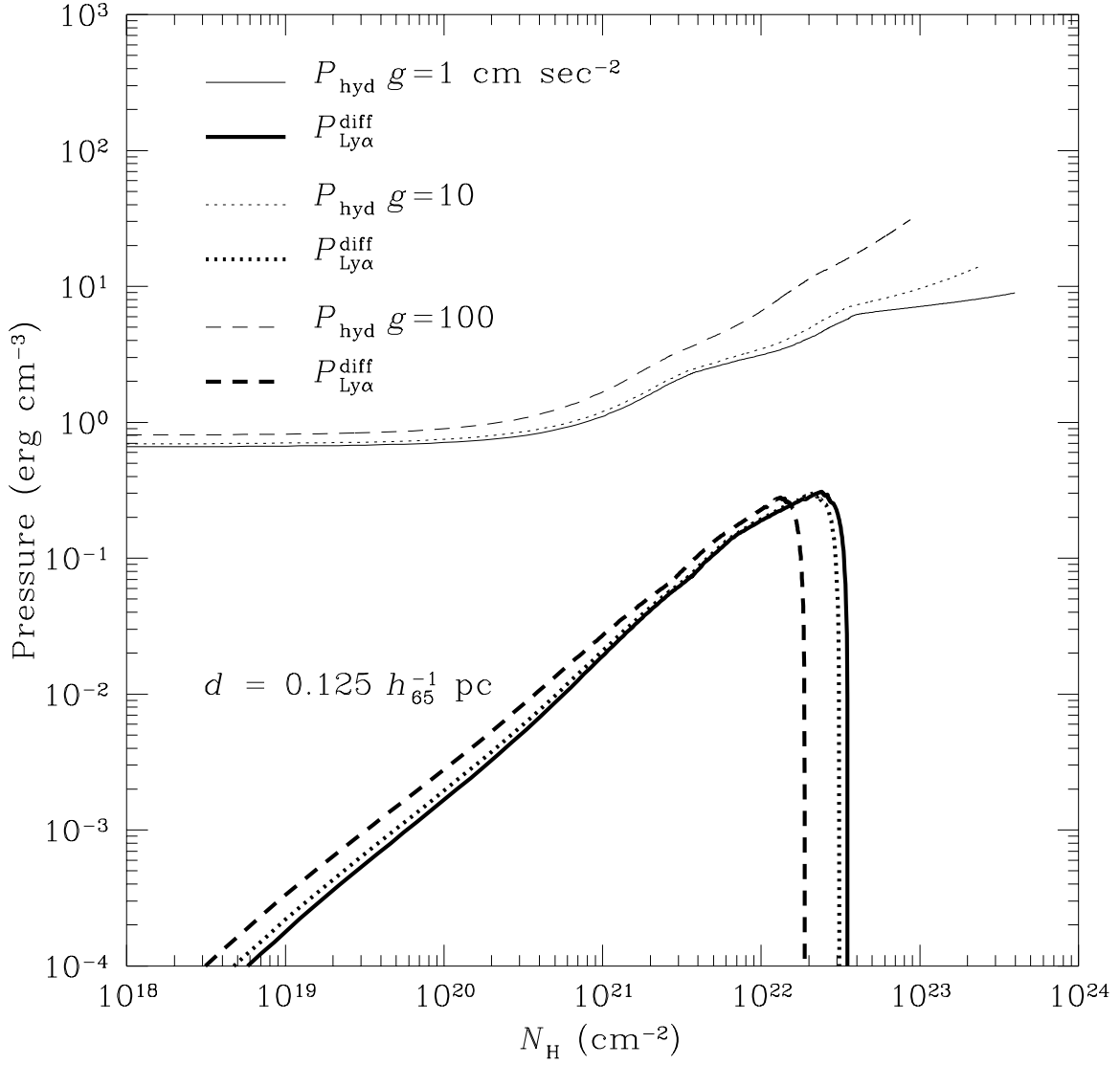


Fig. 4.— Same as Figure 3, but for $A/(4\pi d^2) = 9.47 \times 10^{10} \text{ erg cm}^{-2} \text{ s}^{-1}$, corresponding to a distance $d = 0.125 \ h_{65}^{-1} \text{ pc}$ from an AGN with $L_{46} = 27.8 \ h_{65}^{-2}$.

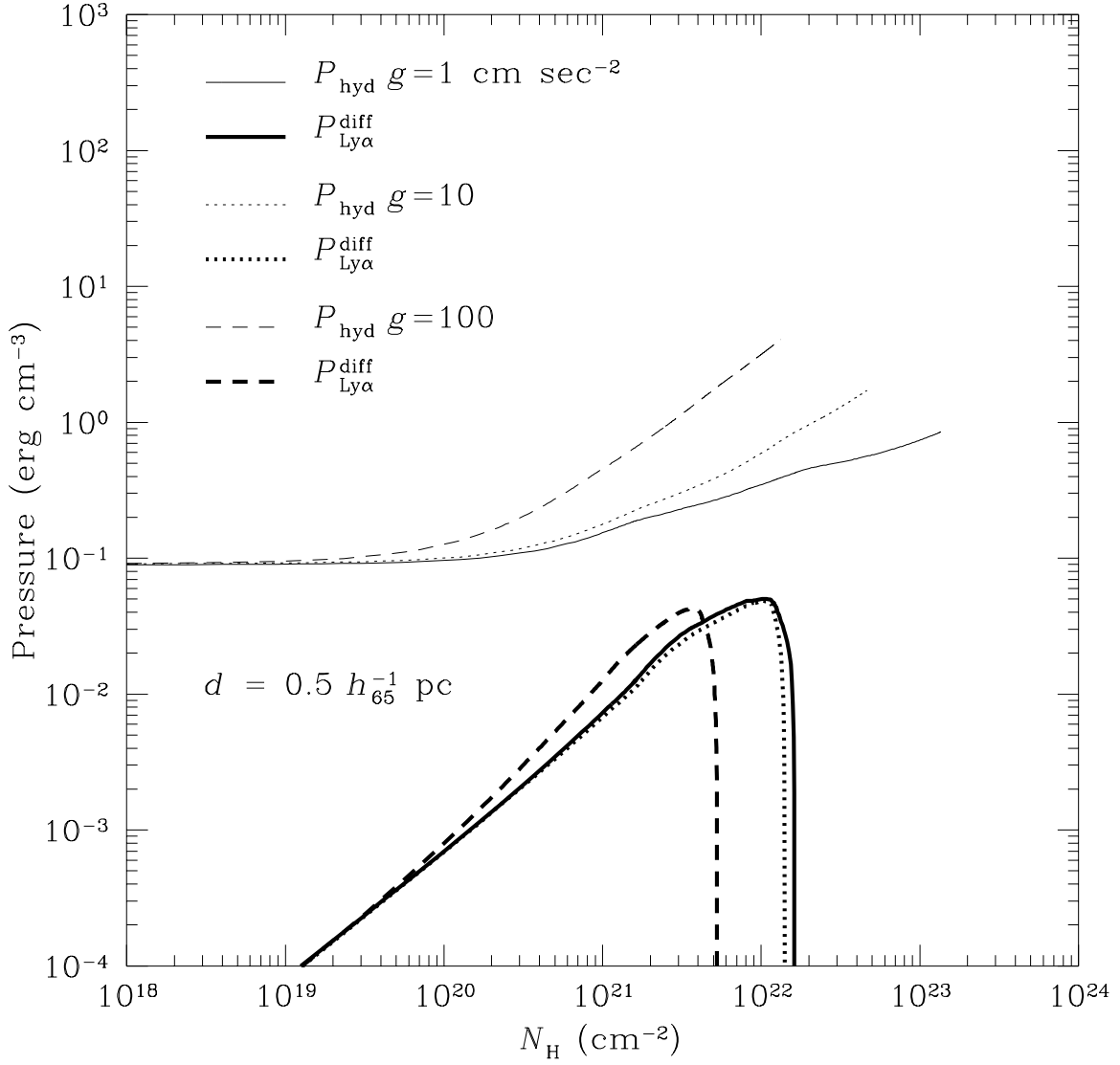


Fig. 5.— Same as Figure 3, but for $A/(4\pi d^2) = 5.92 \times 10^9 \text{ erg cm}^{-2} \text{ s}^{-1}$, corresponding to a distance $d = 0.5 h_{65}^{-1} \text{ pc}$ from an AGN with $L_{46} = 27.8 h_{65}^{-2}$.

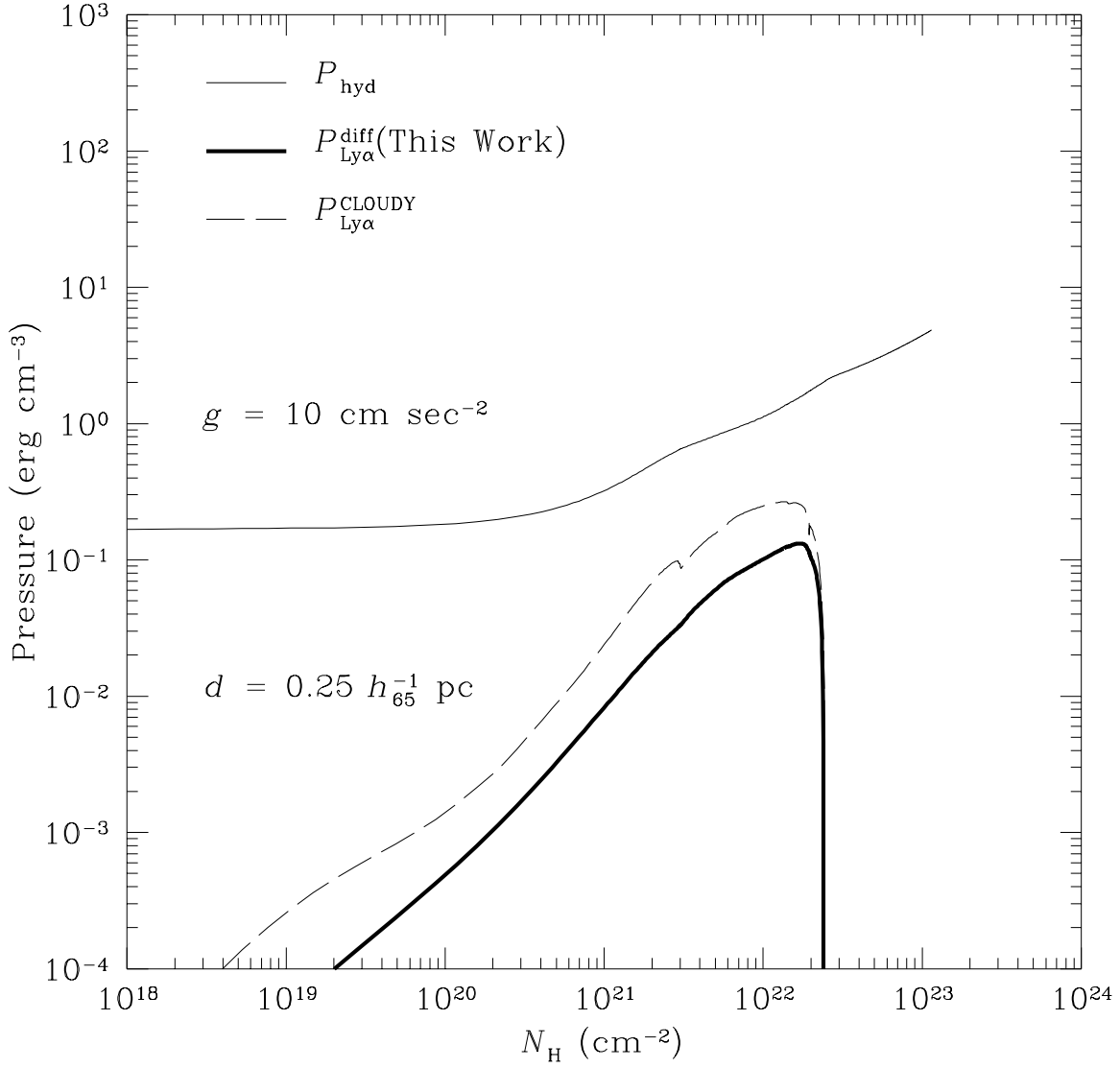


Fig. 6.— Comparison of the Ly α pressure derived from our calculation with that calculated by CLOUDY in the escape probability approximation, for $g = 10 \text{ cm s}^{-2}$, and $A/(4\pi d^2) = 2.37 \times 10^{10} \text{ erg cm}^{-2} \text{ s}^{-1}$ as in Figures 1–3.

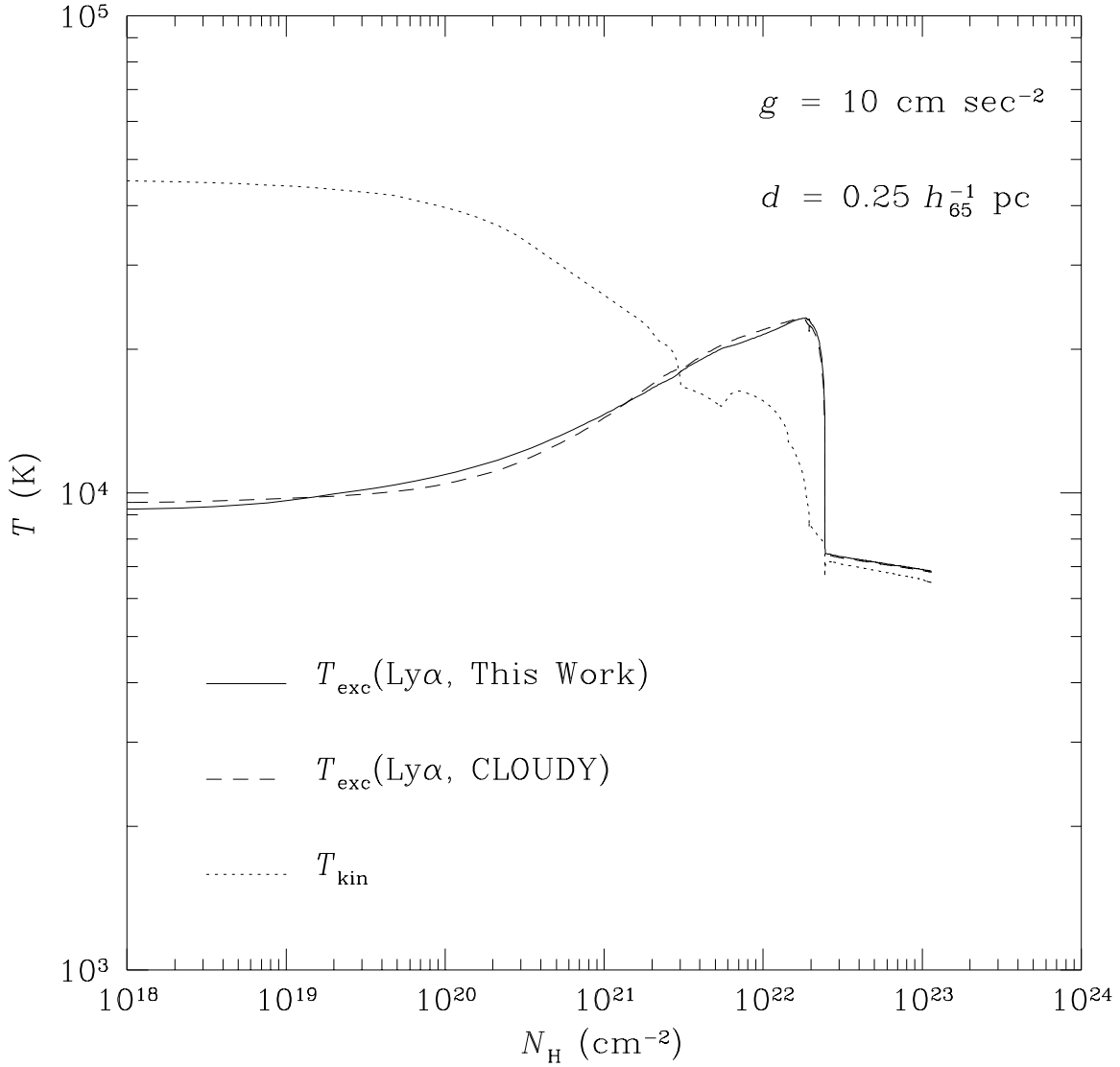


Fig. 7.— Comparison of the excitation temperature T_{exc} in Ly α derived from our calculation with that calculated by CLOUDY in the escape probability approximation, for $g = 10 \text{ cm s}^{-2}$, and $A/(4\pi d^2) = 2.37 \times 10^{10} \text{ erg cm}^{-2} \text{ s}^{-1}$ as in Figures 1–3 and 6. For reference, the kinetic temperature T_{kin} is also given.